1. AGENCY USE ONLY (Leave blank)	2. REPORT DATE	3. REPORT TYPE AND DATES COVERED
	June 26, 1991	

4. TITLE AND SUBTITLE
Static, Microwave, Infrared, and Visible Permittivity Related to chemical Structure: N-methylacetamide, N-dimethyl Acetamide and their Mixtures in CCl_4 at 32°C

5. FUNDING NUMBERS

6. AUTHOR(S)
Paul Firman, Edward M. Eyring, Meizhen Xu, Andrea Marchetti and Sergio Petrucci

7. PERFORMING ORGANIZATION NAME(S) AND ADDRESS(ES)
Weber Research Institute, Polytechnic University, Farmingdale, NY 11735
Department of Chemistry, University of Utah, Salt Lake City, UT 84112

8. PERFORMING ORGANIZATION REPORT NUMBER

9. SPONSORING/MONITORING AGENCY NAME(S) AND ADDRESS(ES)
U. S. Army Research Office
P. O. Box 12211
Research Triangle Park, NC 27709-2211

10. SPONSORING/MONITORING AGENCY REPORT NUMBER
ARO 26636.2-CH

11. SUPPLEMENTARY NOTES
The view, opinions and/or findings contained in this report are those of the author(s) and should not be construed as an official Department of the Army position, policy, or decision, unless so designated by other documentation.

12a. DISTRIBUTION/AVAILABILITY STATEMENT
Approved for public release; distribution unlimited.

12b. DISTRIBUTION CODE

13. ABSTRACT (Maximum 200 words)

Static dielectric permittivities, ϵ_0, and visible refractive indices, n_D (at the sodium doublet λ= 589.3 nm) are reported for N-methylacetamide (NMA), N-dimethylacetamide (DMA), their mixtures with $CC\ell_4$ over a broad concentration range and for NMA-DMA mixtures over a broad range of concentrations at 32°C. UHF and microwave complex permittivities from 0.3 to 90 Ghz and far infrared refractive indices at $\bar{\nu}$ = 130 and $\bar{\nu}$ = 380 cm^{-1} for NMA and their mixtures with $CC\ell_4$ and at $\bar{\nu}$ = 130 cm^{-1} for DMA - $CC\ell_4$ mixtures up to 1 M DMA at 32°C are also reported. Dramatic differences between NMA and DMA in both the static permittivities and relaxation times (for both pure liquids and their mixtures in $CC\ell_4$) are attributed to chain formation through H-bonding for the monosubstituted amides. DMA acts as a kind of "chain-terminator" when added to NMA. The difference in behavior between the two liquids disappears in the cases of infrared permittivities and visible n_D^2 values.

14. SUBJECT TERMS	15. NUMBER OF PAGES
	30
	16. PRICE CODE

17. SECURITY CLASSIFICATION OF REPORT	18. SECURITY CLASSIFICATION OF THIS PAGE	19. SECURITY CLASSIFICATION OF ABSTRACT	20. LIMITATION OF ABSTRACT
UNCLASSIFIED	UNCLASSIFIED	UNCLASSIFIED	UL

NSN 7540-01-280-5500

Standard Form 298 (Rev 2-89)
Prescribed by ANSI Std 239-18
298-102

Static, Microwave, Infrared, and Visible Permittivity Related to Chemical Structure: N-methylacetamide, N-dimethyl Acetamide and their Mixtures in CCl_4 at 32°C

by

Paul Firman, Edward M. Eyring, Meizhen Xu,

Andrea Marchetti and Sergio Petrucci*

Weber Research Institute, Polytechnic University, Farmingdale, NY 11735

and Department of Chemistry, University of Utah, Salt Lake City, UT 84112

Abstract

Static dielectric permittivities, ϵ_o, and visible refractive indices, n_D (at the sodium doublet λ = 589.3 nm) are reported for N-methylacetamide (NMA), N-dimethylacetamide (DMA), their mixtures with $CC\ell_4$ over a broad concentration range and for NMA-DMA mixtures over a broad range of concentrations at 32°C. UHF and microwave complex permittivities from 0.3 to 90 GHz and far infrared refractive indices at $\bar{\nu}$ = 130 and $\bar{\nu}$ = 380 cm^{-1} for NMA and their mixtures with $CC\ell_4$ and at $\bar{\nu}$ = 130 cm^{-1} for DMA - $CC\ell_4$ mixtures up to 1 M DMA at 32°C are also reported. Dramatic differences between NMA and DMA in both the static permittivities and relaxation times (for both pure liquids and their mixtures in $CC\ell_4$) are attributed to chain formation through H-bonding for the monosubstituted amides. DMA acts as a kind of "chain-terminator" when added to NMA. The difference in behavior between the two liquids disappears in the cases of infrared permittivities and visible n_D^2 values.

Introduction

The relation between chemical structure and the static and relaxational dielectric properties of liquids presents a fascinating puzzle to physical chemists. The far infrared frequency region where dipolar rotation has relaxed and the decay of the atomic polarization occurs (and progressing into

the mid-infrared and visible regions) is one of the least studied frequency domains in liquids. Knowledge of chemical structure and dielectric properties in the UHF-microwave region can be used in the design of supercapacitors[1] using liquids (or solid polymers with filling-in liquids) to improve capacitor performance. The value of the permittivity ϵ_∞ at the end of the dipolar rotation dielectric spectrum can also be useful to researchers investigating the picosecond molecular dynamics of liquids.[2] The longitudinal relaxation time τ_L, [believed to be related to the dielectric rotational relaxation time τ_D by relations such as $\tau_L = (\epsilon_\infty/\epsilon_o)\tau_D$] is at times difficult to evaluate because of uncertainty in the value of ϵ_∞.

With these applications in mind, we decided to study the relaxational behavior of the amides and their mixtures with $CC\ell_4$ used as a diluent. Additional interest attaches to the peptide -NH-C = O group contained in these molecules. Whereas a plentitude of vibrational information exists[3] for the amides, few microwave dielectric relaxation results,[4,5] often for a limited frequency range, exist, and no infrared dielectric data, to the knowledge of the present authors, are available.

Static permittivities of monosubstituted and disubstituted amides dissolved in $CC\ell_4$ have been shown[6,7] to give strikingly different behavior. The apparent dipole moment of the monosubstituted amides <u>increases</u> with the concentration of the amide. This was attributed to the formation of H-bonded chains of the type -N - H ••• O = C- between monosubstituted amides. Because of the preponderant trans-configurational orientation of the -N - H group with respect to the -C = O group of the same monosubstituted molecule,[3, 3a] the result was believed to be the formation of chains between contiguous amide molecules. Unsubstituted amides, on the other hand, tend to form rings

between two amides and the net apparent dipole moment decreases with increasing concentration of amide.

Starting from these germinal ideas, the present paper reports first a repetition of the work with NMA, DMA, and their mixtures with $CC\ell_4$ to determine the static permittivity at f = 1.1 MHz. The study has then been extended to the visible frequency range at the D-doublet of sodium (λ = 589.3 nm or $\bar{\nu}$ = 16,969 cm^{-1}, f = 509 THz where 1 THz = 10^{12} Hz).

The difference in behavior of the static permittivities ϵ_o and the relative similarities of the optical permittivities n_D^2 observed upon increasing the concentration of either NMA or DMA in $CC\ell_4$ is striking, confirming the attribution of the differences to H-bonding. Extension of the study to NMA-DMA mixtures confirms that DMA acts as a kind of "chain-terminator" of the NMA chains.

The dynamic properties of DMA-$CC\ell_4$ at microwave and far IR frequencies and of NMA-$CC\ell_4$ at far-IR frequencies are also reported. For both mixtures the microwave permittivities decay continuously to the visible value of n_D^2, the decay of the atomic polarization showing itself as a tail at higher frequency of the Cole-Cole plot depicting the main rotational relaxation locus.

Experimental

The equipment and procedures used to determine the static permittivities, refractive indices (at the sodium D-line doublet), microwave complex permittivities and far infrared refractive indices n_{IR} and attenuation coefficients α, have been described elsewhere.[8] NMA (Aldrich 99+%) was recrystallized five times resulting in a melting point of 30.5°C. DMA (Aldrich 99+%) was distilled in vacuo twice after exposure overnight to P_4O_{10}

and subsequent decantation of the liquid prior to distillation. Carbon tetrachloride (Aldrich 99+%) was purified as described previously.[8]

Solutions were prepared by weight in volumetric flasks. Exposure to the atmosphere during solution preparation and filling of sample cells was limited to 30-60 seconds total.

Results and Discussion

a) Static and Visible Permittivities

Figures 1A and 1B present the static permittivities and the refractive indices n_D (at λ = 589.3 nm) for the DMA-$CC\ell_4$ and for the DMA-$CC\ell_4$ mixtures at 32°C, respectively. Table I (microfilm edition) collects the corresponding data at the compositions (expressed in mol/dm^3) investigated. Detailed dilute ranges for C $\leq$ 1 mol/dm^3 of the polar component for both mixtures for the static permittivities ϵ_o and visible refractive indices n_D for the NMA-$CC\ell_4$ and DMA-$CC\ell_4$ systems at 32°C are shown in Figures 2A and 2B, respectively.

From the Figures it can be seen that nothing significant differentiates the n_D vs composition plots for NMA-$CC\ell_4$ from the corresponding plots for the DMA-$CC\ell_4$ mixtures. On the other hand, the NMA-$CC\ell_4$ mixture permittivities increase much faster with the concentration of the polar component than do the permittivities of the DMA-$CC\ell_4$ mixtures. Also the ϵ_o vs. C_{NMA} plot is nonlinear.

The above empirical observations suggest that the source of the different behavior of ϵ_o and of n_D (or of the optical permittivity $\epsilon' \approx n_D^2$) lies in a phenomenon relevant to static conditions (static in this case meaning at f = 1.1 MHz), and becomes irrelevant or already relaxed at the optical wavelength λ = 589.3 nm (f = 509.1 THz).

We concur with previous observations[6,7] in proposing that the source of the difference in the above described behavior of ϵ_o and n_D^2 vs. composition is H-bonded chain formation in NMA mixtures, a phenomenon absent in the DMA mixtures.

The idea that an increase in the concentration of NMA causes polymeric chains to form with a progressive increase of the apparent dipole moment of the solute, is confirmed in Figure 3A. In this Figure the Böttcher function[9]

$$(\epsilon_o - \epsilon_\infty) = \frac{4\pi LC \times 10^{-3}}{(1 - \alpha f)^2} \cdot \frac{3\epsilon_o}{2\epsilon_o + 1} \cdot \frac{\mu^2}{3kT}$$

rearranged as $f(\epsilon_o) = (\epsilon_o - n_D^2) \frac{2\epsilon_o + 1}{3\epsilon_o}$, is plotted vs. C_{NMA}. [The position $\epsilon_\infty = n_D^2$ taken here will be discussed in Section c, below.]

A continuous change in slope is observed that is presumably attributable to an increase of μ. At low concentrations of NMA ($C_{NMA} < 0.3$ mol/dm^3), linear regression of $f(\epsilon_o)$ vs. C_{NMA}, giving 50% statistical weight to the origin, gives a determination coefficient $r^2 = 0.984$ and $f(\epsilon_o) = -0.037 + 5.50\ C_{NMA}$.

We neglect the quantity αf (the product of the polarizability and the reaction field f) with respect to one, since $(1-\alpha f)$ is of the order of 0.9. Thus we obtain from the slope = 5.50 above, $\mu = 9.5 \times 10^{-18}$ e.s.u. cm as the apparent dipole moment of NMA, at low concentrations in $CC\ell_4$.

Figure 3B is the Böttcher plot of $f(\epsilon_o)$ vs. C_{DMA} for the DMA-$CC\ell_4$ mixtures at 32°C and $C_{DMA} \leq 1$ M. Here the ϵ_∞ values have been calculated from the function

$$\epsilon_\infty = 1.95 + 0.402\ C_{DMA} - 0.0145\ C^2_{DMA}$$

with $r^2 = 0.985$ calculated from the data of Table II and the microwave data of this work (Section b, below).

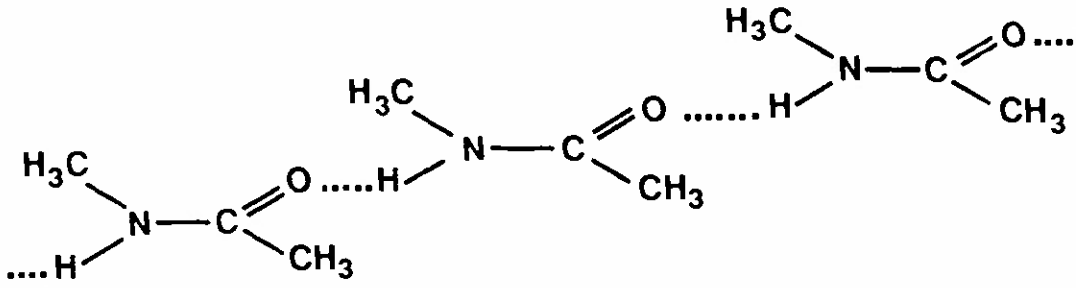
H3C
N
C
O
CH3
H
H3C
N
C
O
CH3
H
H3C
N
C
O
CH3
H

The plot in Figure 3B appears to be linear. Linear regression of $f(\epsilon_o)$ vs. C_{DMA}, assigning 50% statistical weight to the origin, gives a determination coefficient $r^2 = 0.981$ and $f(\epsilon_o) = -0.035 + 1.38_5\ C_{DMA}$. From this result and from $1.38_5 = 4\pi L \times 10^{-3}\ (\mu^2/3kT)$, we calculate $\mu = 4.8 \times 10^{-18}$ e.s.u. cm, namely a value smaller by a factor of two than the μ noted above for NMA.

The continuous change in slope apparent in Figure 3A suggests that even at concentrations of the order of $C_{NMA} \simeq 0.3$ M significant amounts of dimer and polymer chains of the type

have been formed. No such dimers and polymers can form in DMA-$CC\ell_4$ mixtures.

This point is taken again in the study of NMA-DMA mixtures at 32.0°C. Specifically, it is conceivable that by adding DMA to NMA, the chains present with DMA would be shortened and interrupted each time a molecule of DMA takes part in the chain by forming a hydrogen bond with an NMA molecule. DMA would then act as a kind of chain terminator to NMA. The dielectric consequences of this addition should be a strong nonlinearity of the static permittivity of the mixture as a function of C_{NMA}. This is evident in Figure 4 that presents ϵ_o vs. C_{NMA} at 32.0°C. A strong nonlinearity of the plot contrasts with Figure 1A that shows only a relatively mild nonlinearity for the NMA-$CC\ell_4$ mixtures at 32.0°C. Presumably, $CC\ell_4$ only dilutes NMA, especially near pure NMA where the chain length is comparable to that in pure NMA. On the other hand, DMA appears to disrupt the chain structure of NMA much more abruptly.

b) Microwave Complex Permittivities

In this section we will explore the frequency response of the complex permittivity $\epsilon^* = \epsilon' - J\epsilon''$ (with ϵ' the real coefficient and with ϵ'' the coefficient of the imaginary part of ϵ^*) for the systems NMA, DMA and the DMA-$CC\ell_4$ mixtures at 32°C.

Figure 5A presents literature data[4] for f = 0.05 to f = 0.220 GHz at 31.4°C, data[5] from f = 0.450 to f = 2.0 GHz at 31°C and data from the present work from f = 8.33 to f = 89.35 GHz in addition to the static value of ϵ_o at f = 1.1 MHz, all at 32.0°C. The solid line is the Debye single relaxation function with parameters $\epsilon_o = 177$, $\epsilon_\infty = 4$ and $f_r = 0.257$ GHz as proposed by Omar.[5] The fit appears to be in reasonable agreement with the data with the exception of the point at f = 50 MHz. The fit is supported by the static value $\epsilon_o = 176.3$ of the permittivity at 32°C. The fact that some of the data were obtained at 31°C and some at 32°C does not appear to be significant. Notice, however, (Figure 5B) that the Debye fit with $\epsilon_\infty = 4$ is not satisfactory for the points above f ≃ 30 GHz, with a tail going toward n_D^2 (the value of the permittivity at the sodium line) being evident.

In Figure 5B the infrared value of ϵ' and ϵ'' at f = 11.4 THz is taken from the data of Table III, discussed in Section c below.

The presence of a tail in the Cole-Cole plot at high frequencies in the far-infrared region, has already been noted for benzonitrile in our previous work.[8] The phenomenon appears to be related to the librational resonant relaxation of dipoles and induced dipoles handled by preliminary theories reviewed by Madden and Kivelson.[10]

Next we consider the DMA data at 32°C, presented as a Cole-Cole locus plot of ϵ'' vs. ϵ' in Figure 6A. A single Debye relaxation function with

parameters $\epsilon_o = 37.20$, $\epsilon_\infty = 4.5$ and $f_r = 12$ CHz seems adequate to describe the data (solid line in Figure 6A). It is unfortunate that many resonant bands in the far-IR spectrum of DMA prevent us from filling the gap between f = 89.5 CHz and n_D^2. Only data for the mixtures DMA-$CC\ell_4$ at $C_{DMA} \leq 1$ M could be collected as discussed in Section c, below.

Figures 6B and 6C report the ϵ'' vs. ϵ' plot of mixtures of DMA-$CC\ell_4$ at molar concentration of DMA C = 8.51 M and C = 6.00 M respectively at 32.0°C. Similar plots are shown in Figures 7A, 7B and 7C for DMA concentrations of C = 4.00, C = 2.00 and C = 1.00 M respectively and 32.0°C. A single Debye relaxation appears to describe the above data of Fig. 7 up to 30 - 50 CHz within experimental error for the DMA-$CC\ell_4$ mixtures of $C_{DMA} = 4.00$ and $C_{DMA} = 2.00$ M at 32.0°C.

Table II (microfilm edition) reports the values of the relaxation parameters used to fit the data for the DMA-$CC\ell_4$ mixtures. From Table II it appears that there is a minimum with composition of the relaxation frequency (or a maximum with composition of the relaxation time since $\tau^{-1} = 2\pi f_r$) for the DMA-$CC\ell_4$ mixtures at 32.0°C. This is shown in Figure 8.

c) Far-Infrared Refractive Indices and Attenuation Constants

The values of the refractive indices n in the infrared at $\bar{\nu} = 380$ cm^{-1} (f = 11.4 THz), the value of the attenuation constant α (neper cm^{-1}), and the calculated values of the real part ϵ' and of the coefficient ϵ'' of the imaginary part of the complex permittivity $\epsilon^* = \epsilon' - J\epsilon''$ are all presented in Table III (microfilm edition) for the NMA-$CC\ell_4$ mixtures at 32°C.

Given that $n = \lambda_o/\lambda$, $\epsilon' = \left(\frac{\lambda_o}{\lambda}\right)^2 \left[1 - \left(\frac{\alpha\lambda}{2\pi}\right)^2\right]$, and $\epsilon'' = \left(\frac{\lambda_o}{\lambda}\right)^2 \frac{\alpha\lambda}{\pi}$, from the values of n, α and λ_o at f = 11.4 THz, the

quantities ϵ' and ϵ'' can be calculated. At this frequency it is found that $n^2 \approx \epsilon'$ within experimental error.

Figures 9A through 9F show the value of ϵ' and of n^2 extending over the range from 8 GHz (X-band) at microwave frequencies down to the visible (D-doublet of sodium). The data seem to correlate smoothly over the entire range investigated, showing with some large gaps of unknown behavior an apparent monotonic decrease of ϵ' and n^2 with frequency. This reflects the decay of the atomic polarization of the NMA molecules possibly associated with phenomena such as dipole libration as predicted by Hill[11] and dipole libration and induced dipole interactions as discussed more recently by Madden and Kivelson.[10]

In Section a above, we discussed the apparent change of the dipole moment of NMA with concentration for the NMA-$CC\ell_4$ mixtures using the Böttcher equation and the position $\epsilon_\infty = n_D^2$, namely the squared visible refractive index. We were concerned that by doing so, we had included the decay of the atomic polarization together with that related to the dipole rotation in the Böttcher expression. We have then measured both refractive index n and attenuation constant α at the wave number $\bar{\nu} = 130$ cm^{-1} (f = 3.90 THz) because of the existence of a window in the infrared spectrum of NMA and of the NMA-$CC\ell_4$ mixtures at wave numbers between approximately 110 and 220 cm^{-1}. The results are collected in Table IV (microfilm edition) and Figure 10A for concentrations in NMA $C_{NMA} \leq 1$ M. The averaged squared refractive index at this frequency is $\bar{n}^2 = 2.18 \pm 0.04$. From Table I, in the concentration range 0 to 1 M, the visible (Na-doublet) squared refractive index is calculated to be in the range 2.11 to 2.04, namely on the average 5% lower than at the far-IR frequency of 3.9 THz. Reiterating this point, from Figure 9A at f $\approx$ 100

GHz the value of $\epsilon' \approx 2.2_7$ for the concentration C_{NMA} = 1.19 M. Furthermore, the values of ϵ' are still decreasing from frequencies f < 100 GHz (Fig. 9A). The value at $\bar{\nu}$ = 130 cm^{-1} at about this concentration, C_{NMA} = 1 M, is n^2 = 2.13 ± 0.06 (Table IV) whereas at $\bar{\nu}$ = 380 cm^{-1} (f = 11.4 THz), (Table III) n^2 = 2.14 and in the visible (λ = 589.3 nm) n_D^2 = 2.04. It appears, therefore, that using n_D^2 will cause an error of less than 10% in ϵ_∞. Given the rapid increase in ϵ_o with composition for the mixture NMA-$CC\ell_4$, the curvature in Figure 3A is not an artifact arising from errors involved in using n_D^2 for ϵ_∞ in the Böttcher function.

For the DMA-$CC\ell_4$ mixtures the refractive indices n and the attenuation constants α at the wave number $\bar{\nu}$ = 130 cm^{-1} (f = 3.9 THz) were also measured. A transparent window in the infrared spectrum also exists in this region for DMA although some small bands interfere making the fringe method[8] used to measure n inadequate at $C_{DMA} \geq 1$ M. Table IV and Figure 10B report the values of n, α, $\epsilon' \approx n^2$ and ϵ'' for the DMA-$CC\ell_4$ mixtures of $C_{DMA} \leq 1$ M at 32°C and $\bar{\nu}$ = 130 cm^{-1}.

The average value of the squared refractive index at this frequency and concentrations ranging from 0 to 1 M is n^2 = 2.22 ± 0.02. From Table I the corresponding squared-sodium line-refractive index is calculated to be in the range 2.11 to 2.05. We have repeated the calculation with the Böttcher function using $\epsilon_\infty = n_D^2$ to see the effect of this approximation in the calculated value of the apparent dipole moment μ of DMA, already done with the extrapolated values of ϵ_∞ (Figure 3B).

Values of $f(\epsilon) = (\epsilon_o - n_D^2) \frac{2\epsilon_o + 1}{3\epsilon_o}$ were calculated. Linear regression

of $f(\epsilon)$ vs. C_{DMA}, giving 50% statistical weight to the origin, yielded $r^2 = 0.991$ and $f(\epsilon) = 0.024 + 1.53_1\ C_{DMA}$ from which, since $1.53 = 4\pi L \times 10^{-3}\ \mu^2/3kT$, the value of $\mu = 5.0_5 \times 10^{-18}$ e.s.u. cm was calculated.

This figure is about 4% higher than the value $\mu = 4.8 \times 10^{-18}$ e.s.u. cm calculated using the extrapolated ϵ_∞ values from the microwave region and the Debye function. The two figures $\mu = 5.0_5$ and $\mu = 4.8_1 \times 10^{-18}$ e.s.u. cm are within experimental error of the slope of the Böttcher plot. This lends indirect credence to the idea that for the NMA-$CC\ell_4$ mixtures the Böttcher plot gives a real curvature (and not an artifact due to the use of n_D^2), hence a real change in the apparent value of μ with composition. It is unfortunate that our equipment does not permit measurements in the 10 to 300 MHz range of complex permittivity at radio frequencies, where the relaxation locus of the NMA-CCl_4 mixtures probably exists.

Acknowledgments: The authors wish to express their thanks to the A.R.O., Durham, N.C., grant # DAAL03-89-K-0148, for support of this work.

References

1. U. S. Army Workshop on Capacitors for Pulse Power Application, Ashbury Park, N.J., Nov. 17-19 (1987).

2. Maroncelli, M.; Fleming, G.R. J. Chem. Phys. 1988, *89*, 875; Kahlow, M.A.; Jarzeba, W.; Kang, T.J.; Barbara, P. F. J. Chem. Phys. 1989, *90*, 151.

3. Hallam, H.E.; Jones, C.M. J. Mol. Structure 1970, *5*, 1 and previous literature contained in this review article; Klotz; I.M.; Franzen, J.S. J. Am. Chem. Sec. 1962, *84*, 3461; Baron, M.H.; deLoze, C.; Sagon, G. J. Chimie Physique 1973, *70*, 1509.

3a. LaPlanche, L.A.; Rogers, M.T. J. Am. Chem. Soc. 1964, *86*, 337.

4. Bass, S.J.; Nathan, W.I.; Meighan, R.M.; Cole, R.H. J. Phys. Chem. 1964, *68*, 509.

5. Omar, N.M. J. Chem. Soc. Faraday I 1980, *76*, 711.

6. Bates, W. W.; Hobbs, M.E. J. Am. Chem. Soc. 1952, *74*, 746.

7. Worsham, J.E., Hobbs, M.E., J. Am. Chem. Soc. 1954, *76*, 206.

8. Firman, P.; Marchetti, A; Xu, M.; Eyring, E.M.; Petrucci, S. J. Phys. Chem., in press.

9. Bōttcher, C.J.F. Theory of Electrical Polarization, 2nd Ed., Elsevier Amsterdam, 1973.

10. Madden, P.A.; Kivelson, D., in Vol. LVI, "Advances in Chemical Physics", Prigogine, I.; Rice, S.A., Editors, John Wiley and Sons, N.Y., 1984 and literature quoted therein.

11. Hill, N.E. Proc. Phys. Soc. 1963, *82*, 723.

Table I (microfilm edition)

Static permittivity ϵ_o (f=1.1 MHz) and optical refractive index n_D (λ=589.3 nm) for NMA-CCl_4, DMA-CCl_4 and DMA-NMA mixtures at 32.0°C and the compositions investigated (expressed in mole fractions X and molarity C of the polar component).

System: NMA-CCl_4

X_{NMA}	C_{NMA}	ϵ_o	n_D
0.00	0.00	2.25	1.4529_6
0.00555	0.0578	2.40	1.4529_1
0.00989	0.102	2.58	1.4527_0
0.0148	0.153	3.03	1.4526_9
0.0196	0.203	3.53	1.4526_8
0.0289	0.300	4.43	1.4524_9
0.0385	0.401	5.63	1.4524_0
0.0507	0.528	6.90	
0.0575	0.601	7.87	1.4521_6
0.0721	0.752	9.89	
0.0764	0.801	10.77	1.4518_9
0.113	1.193	15.72	1.4508_7
0.163	1.736	22.25	
0.188	2.021		1.4505_2
0.226	2.447	31.83	
0.302	3.320		1.4488_9
0.319	3.506	45.54	1.4479_1
0.405	4.581		1.4468_5
0.465	5.290	64.68	
0.508	5.787		1.4445_9
0.597	7.010		1.4425_6
0.605	7.178	88.95	
0.705	8.50	108.0	1.4382_0
0.797	9.88	123.6	
0.805	9.95		1.4359_3
0.908	11.48	148.9	1.4317_5
0.941	12.05		1.4308_1
1.000	13.09	176.3	1.4284_5

Table I (continued)

System: DMA-$CC\ell_4$

X_{DMA}	C_{DMA}	ϵ_o	n_D
0.00	0.00	2.25	1.4529_6
0.00931	0.096		1.4528_1
0.0145	0.149	2.48	1.4525_8
0.0206	0.212		1.4527_8
0.0290	0.300	2.84	1.4524_7
0.0385	0.400	3.04	1.4524_2
0.0483	0.501	3.21	1.4526_0
0.0514	0.530		1.4525_4
0.0580	0.601	3.30	
0.0588	0.605		1.45251
0.0678	0.701	3.46	1.45250
0.0773	0.801	3.74	1.4523_5
0.0870	0.901	3.93	1.4523_4
0.102	1.06	4.33	1.4522_6
0.304	3.189	9.74	1.4511_4
0.460	4.848	15.16	1.4486_2
0.603	6.383	19.93	1.4456_8
0.644	6.852	21.85	
0.753	7.978		1.4416_3
0.817	8.725	29.18	
0.902	9.663		1.4366_0
0.913	9.745	33.40	
1.000	10.76	37.20	1.4328_4

Table I (continued)

System: DMA-NMA

X_{DMA}	C_{NMA}	ϵ_o	n_D
0	0	37.20	1.4328_4
0.0472	0.5077	39.94	
0.0989	1.075	42.27	1.4327_5
0.159	1.755	44.87	
0.176	1.956	48.79	1.4325_5
0.303	3.444	55.56	1.4321_6
0.512	6.018	74.92	1.4312_9
0.646	7.825	95.13	1.4305_5
0.710	8.653	103.49	1.4303_5
0.806	10.06	121.68	1.4294_0
0.898	11.44	144.39	1.4290_7
1	13.09	176.28	1.4284_5

Table II (microfilm edition)

Relaxation parameters ϵ_o, ϵ_∞ and f_r used to fit the complex permittivity of the DMA-$CC\ell_4$ mixtures at 32.0°C, according to a single Debye relaxation function. Relaxation times (decay of dielectric polarization) $\tau = (2\pi f_r)^{-1}$

X_{DMA}	C_{DMA} (mol/dm^3)	ϵ_o	ϵ_∞	f_r (CHz)	τ (ps)
1.00	10.7_6	37.2	4.5	12	13.3
0.79_8	8.51	27.2	4.5	8.5	18.7
0.56_6	6.00	18.6	3.8	8.5	18.7
0.381	4.00	12.3	3.2	9.0	17.7
0.192	2.00	6.68	2.7	10	15.9
0.096	1.00	4.26	2.3_8	13	12.2

$\epsilon_\infty = 1.95 + 0.402\ C - 0.0145\ C^2$ $\qquad r^2 = 0.985$

Table III (microfilm edition)

Refractive index n, attenuation constant α (neper cm^{-1}), coefficients of the complex permittivity $\epsilon^* = \epsilon' - J\epsilon''$ for NMA-$CC\ell_4$ mixtures at 32°C and $\bar{\nu}$ = 380 cm^{-1} (f = 11.4 THz)

X_{NMA}	C_{NMA} (mol/dm^3)	n	α (cm^{-1})	n^2	ϵ'	ϵ''
1.00	13.09	1.45_4	21.8_2	2.11	2.11	0.0266
0.902	11.48	1.45_8	18.40	2.13	2.13	0.0225
0.707	8.50	1.47_7	17.40	2.18	2.18	0.0215
0.614	7.18	1.47_6	13.96	2.18	2.18	0.0173
0.463	5.29	1.461	10.14	2.14	2.14	0.0124
0.318	3.51	1.530	8.01_0	2.34	2.34	0.0103
0.114	1.19	1.462	3.48_0	2.14	2.14	0.00426

Table IV (microfilm edition)

Refractive index n and attenuation constant α (neper cm^{-1}) and coefficients of the complex permittivity $\epsilon^* = \epsilon' - J\epsilon''$ for NMA-$CC\ell_4$ mixtures and for DMA-$CC\ell_4$ at 32°C and $\bar{\nu}$ = 129.9 cm^{-1} (f = 3.90 THz)

X_{NMA}	C_{NMA} (mol/dm^3)	n	α (cm^{-1})	n^2	ϵ'	ϵ''
0.00	0.00	1.486	2.806	2.21±0.03	2.21	0.0102
0.0289	0.300	1.470	3.493	2.16±0.04	2.16	0.0126
0.0507	0.528	1.491	5.421	2.22±0.04	2.22	0.0198
0.0761	0.801	1.476	6.460	2.18±0.04	2.18	0.0234
0.100	1.060	1.461	12.24	2.13±0.06	2.13	0.0483

$n^2 = 2.21 - 0.055\ C_{NMA}$ $\qquad r^2 = 0.39$

$\alpha = 3.011 - 1.849\ C_{NMA} + 9.530\ C_{NMA}^2$ $\qquad r^2 = 0.960$

X_{DMA}	C_{DMA} (mol/dm^3)	n	α (cm^{-1})	n^2	ϵ'	ϵ''
0.00	0.00	1.486	2.806	2.21±0.03	2.21	0.0102
0.029	0.30_2	1.495	2.351	2.23±0.07	2.23	0.00861
0.0485	0.50	1.490	3.336	2.22±0.04	2.22	0.0122
0.0675	0.70	1.497	4.964	2.24±0.03	2.24	0.0182
0.0962	1.00	1.485	5.745	2.21±0.04	2.21	0.0209

$n^2 = 2.22 - 3.5 \times 10^{-3}\ C$ $\qquad r^2 = 0.01$

$\alpha = 2.57_o + 0.0909\ C_{DMA} + 3.343\ C_{DMA}^2$

Figure Captions

Fig. 1A. Static permittivities ϵ_o and optical refractive indices n_D (at λ = 589.3 nm) plotted versus concentration (mol dm^{-3}) of N-methylacetamide (NMA) in NMA-$CC\ell_4$ mixtures at 32.0°C.

Fig. 1B. Static permittivities ϵ_o and optical refractive indices n_D plotted versus concentration of N-dimethylacetamide (DMA) for DMA-$CC\ell_4$ mixtures at 32.0°C.

Fig 2A. Static permittivities ϵ_o and optical refractive indices n_D versus concentrations of NMA under 1 mol dm^{-3} for NMA-$CC\ell_4$ mixtures at 32.0°C.

Fig. 2B. Static permittivities ϵ_o and optical refractive indices n_D versus concentrations of DMA under 1 mol dm^{-3} for DMA-$CC\ell_4$ mixtures at 32.0°C.

Fig. 3A. Böttcher plot for NMA-$CC\ell_4$ mixtures at 32.0°C.

Fig. 3B. Böttcher plot for DMA-$CC\ell_4$ mixtures at 32.0°C.

Fig. 4 Static permittivities ϵ_o and optical refractive indices n_D versus NMA concentration for DMA-NMA mixtures at 30°C.

Fig. 5A. Cole-Cole plot for N-methylacetamide.

Fig. 5B. Tail of the Cole-Cole plot for N-methylacetamide.

Fig. 6A. Cole-Cole plot for N-dimethylacetamide.

Fig. 6B. Cole-Cole plot for a DMA-$CC\ell_4$ mixture in which the DMA concentration is 8.51 mol dm^{-3} and X_{DMA} = 0.798.

Fig. 6C. Cole-Cole plot for a DMA-$CC\ell_4$ mixture in which the DMA concentration is 6.00 mol dm^{-3} and X_{DMA} = 0.566.

Fig. 7A. Cole-Cole plot for a DMA-$CC\ell_4$ mixture in which the DMA concentration is 4.00 mol dm^{-3} and X_{DMA} = 0.381

Fig. 7B. Cole-Cole plot for a DMA-$CC\ell_4$ mixture in which the DMA concentration is 2.00 mol dm^{-3} and X_{DMA} = 0.192.

Fig. 7C. Cole-Cole plot for a DMA-$CC\ell_4$ mixture in which the DMA concentration is 1.00 mol dm^{-3} and X_{DMA} = 0.096.

Fig. 8. Dielectric relaxation time τ versus the molar concentration of DMA for DMA-$CC\ell_4$ mixtures at 32.0°C.

Fig. 9A. Dielectric permittivity ϵ' (open circles) and squared refractive indices n^2 (dark circles) at microwave, infrared and visible frequencies for NMA-$CC\ell_4$ mixtures at 32°C. C_{NMA} = 1.19M.

Fig. 9B. Same as in 9A. C_{NMA} = 3.51 M.

Fig. 9C. Same as in 9A. C_{NMA} = 5.29 M.

Fig. 9D. Same as in 9A. C_{NMA} = 7.18 M.

Fig. 9E. Same as in 9A. C_{NMA} = 11.48 M.

Fig. 9F. Same as in 9A. C_{NMA} = 13.09 M.

Fig. 10A. Squared refractive indices n^2_{130} and attenuation constants $\alpha_{130}(cm^{-1})$ at $\bar{\nu}$ = 129.9 cm^{-1}(f = 3.90 THz) for NMA in $CC\ell_4$ versus the concentration of NMA (mol dm^{-3}) at 32°C.

Fig. 10B. Squared refractive indices n^2_{130} and attenuation constants $\alpha_{130}(cm^{-1})$ at $\bar{\nu}$ = 129.9 cm^{-1}(f = 3.90 THz) for DMA in $CC\ell_4$ versus the concentration of DMA (mol dm^{-3}) at 32°C.

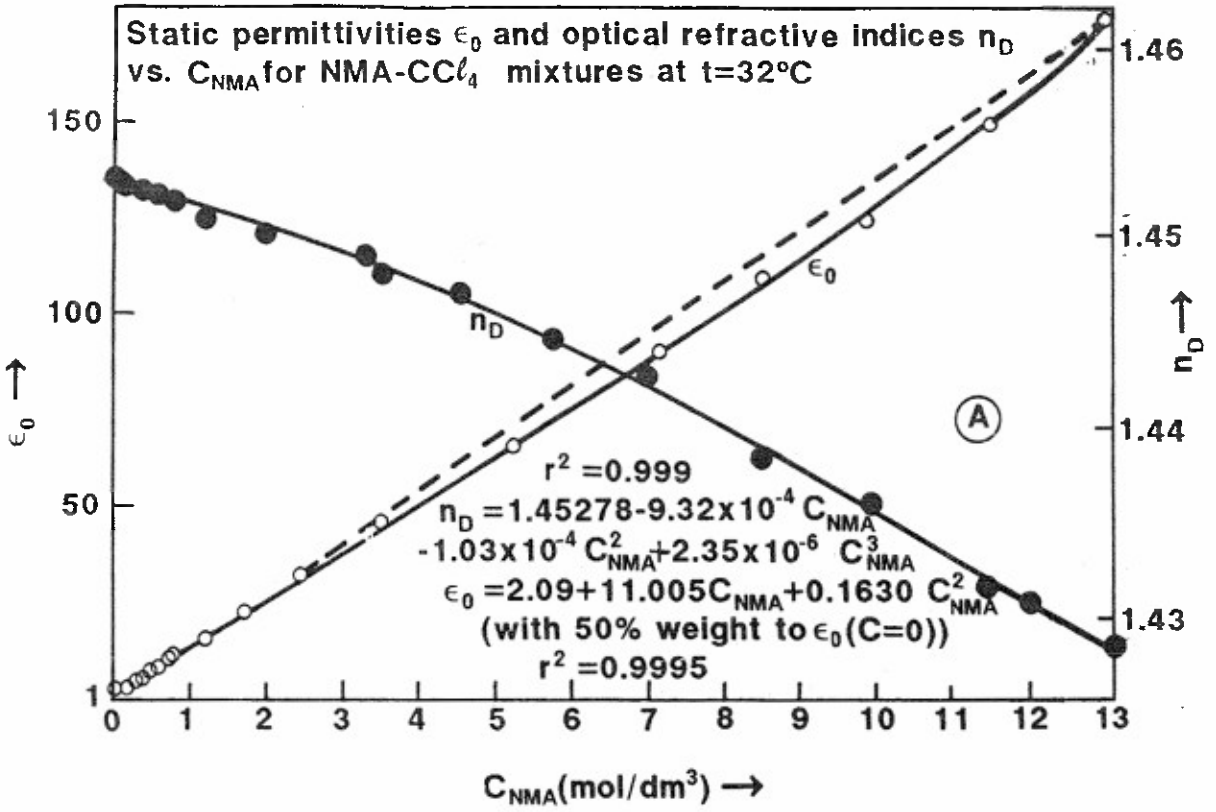
Static permittivities ϵ_0 and optical refractive indices n_D vs. C_{NMA} for NMA-$CC\ell_4$ mixtures at t=32°C
ϵ_0
n_D
A
r^2 =0.999
n_D =1.45278-9.32x10^{-4} C_{NMA}
-1.03x10^{-4} C^2_{NMA}+2.35x10^{-6} C^3_{NMA}
ϵ_0 =2.09+11.005C_{NMA}+0.1630 C^2_{NMA}
(with 50% weight to ϵ_0(C=0))
r^2 =0.9995
C_{NMA}(mol/dm^3) →

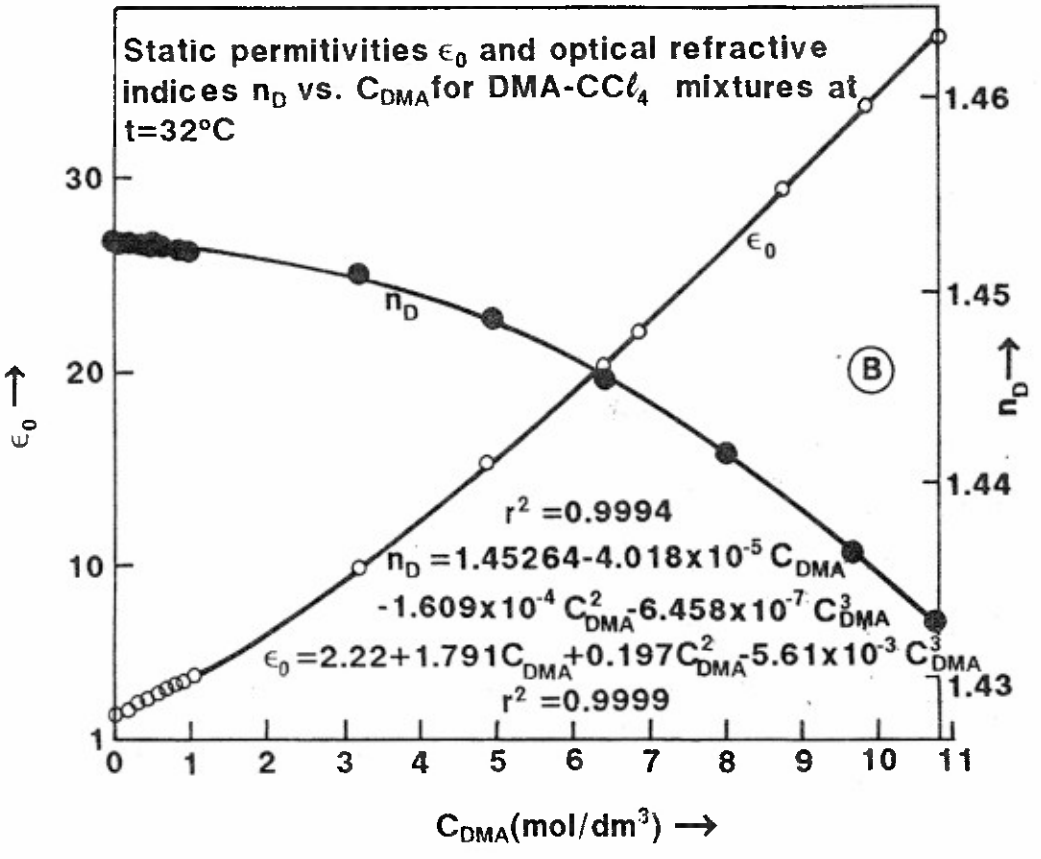
Static permittivities ϵ_0 and optical refractive indices n_D vs. C_{DMA} for DMA-$CC\ell_4$ mixtures at t=32°C
ϵ_0
n_D
B
r^2 =0.9994
n_D =1.45264-4.018x10^{-5} C_{DMA}
-1.609x10^{-4} C^2_{DMA}-6.458x10^{-7} C^3_{DMA}
ϵ_0 =2.22+1.791C_{DMA}+0.197C^2_{DMA}-5.61x10^{-3} C^3_{DMA}
r^2 =0.9999
C_{DMA}(mol/dm^3) →

Fig. 1

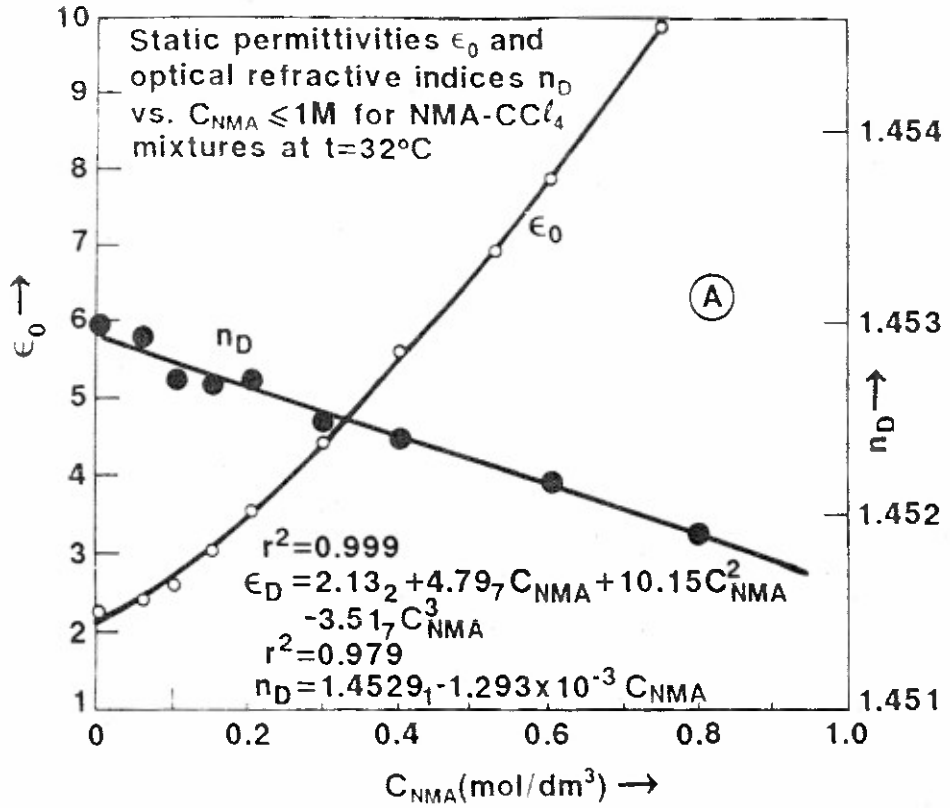
Static permittivities ϵ_0 and optical refractive indices n_D vs. $C_{NMA} \leq 1M$ for NMA-$CC\ell_4$ mixtures at t=32°C
A
ϵ_0
n_D
$r^2=0.999$
$\epsilon_D = 2.13_2 + 4.79_7 C_{NMA} + 10.15 C^2_{NMA} - 3.51_7 C^3_{NMA}$
$r^2=0.979$
$n_D = 1.4529_1 - 1.293 \times 10^{-3} C_{NMA}$
$\epsilon_0 \rightarrow$
$n_D \rightarrow$
$C_{NMA}(mol/dm^3) \rightarrow$

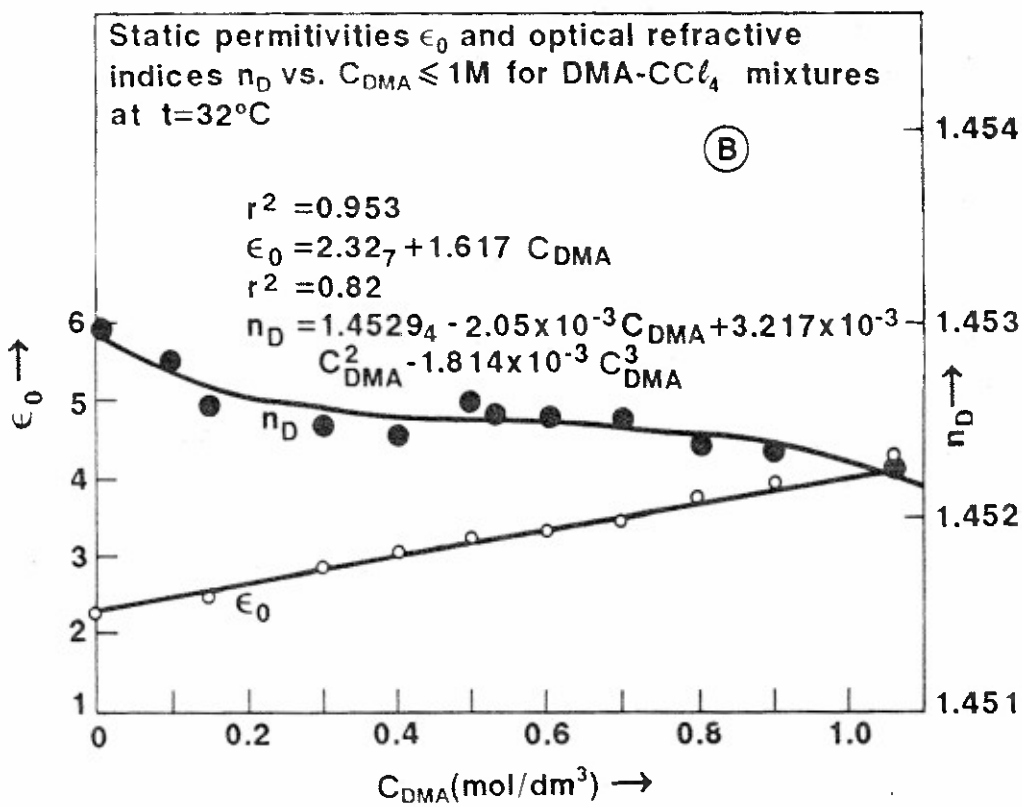
Static permittivities ϵ_0 and optical refractive indices n_D vs. $C_{DMA} \leq 1M$ for DMA-$CC\ell_4$ mixtures at t=32°C
B
$r^2 = 0.953$
$\epsilon_0 = 2.32_7 + 1.617\ C_{DMA}$
$r^2 = 0.82$
$n_D = 1.4529_4 - 2.05 \times 10^{-3} C_{DMA} + 3.217 \times 10^{-3} C^2_{DMA} - 1.814 \times 10^{-3} C^3_{DMA}$
n_D
ϵ_0
$\epsilon_0 \rightarrow$
$n_D \rightarrow$
$C_{DMA}(mol/dm^3) \rightarrow$

Fig. 2

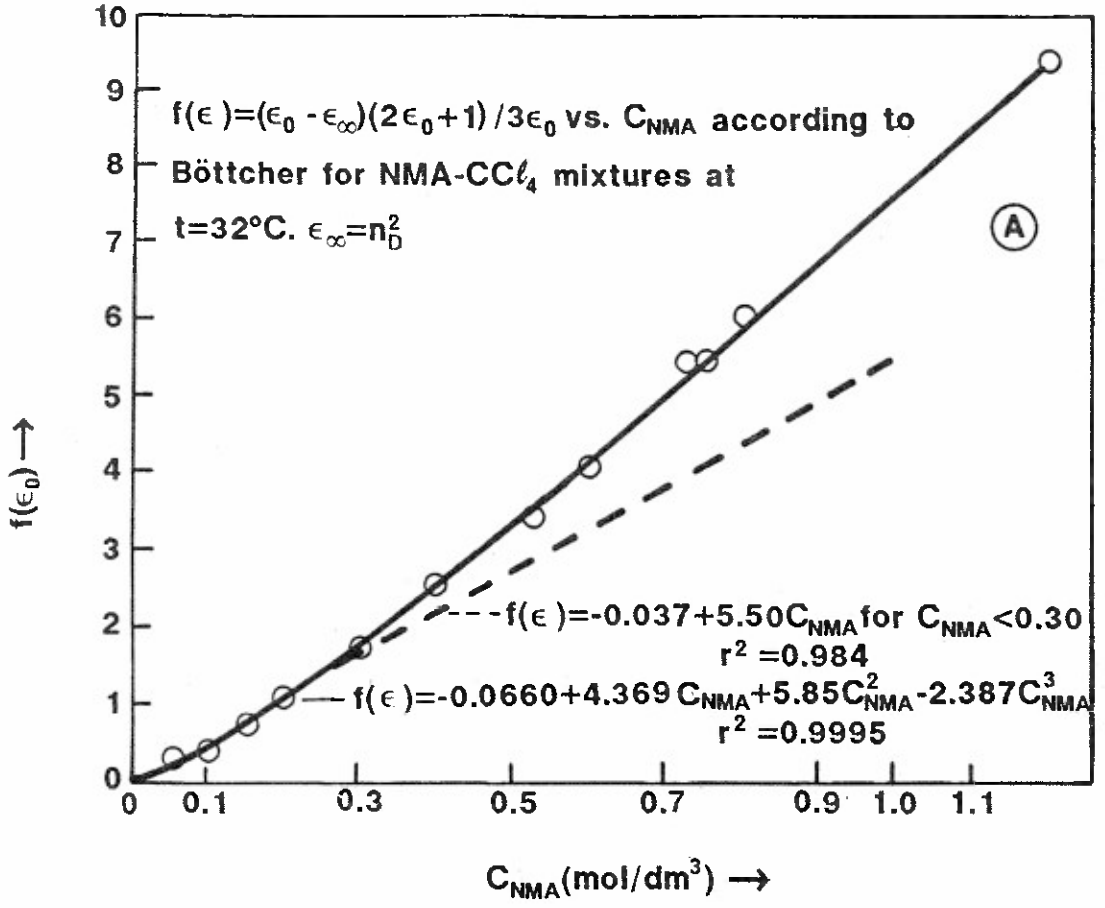
f(ϵ)=(ϵ0 - ϵ∞)(2ϵ0+1) /3ϵ0 vs. CNMA according to
Böttcher for NMA-CCℓ4 mixtures at
t=32°C. ϵ∞=nD2
A
---f(ϵ)=-0.037+5.50CNMA for CNMA<0.30
r2 =0.984
— f(ϵ)=-0.0660+4.369 CNMA+5.85CNMA2-2.387CNMA3
r2 =0.9995
f(ϵ0) →
CNMA(mol/dm3) →
0
0.1
0.3
0.5
0.7
0.9
1.0
1.1
1
2
3
4
5
6
7
8
9
10

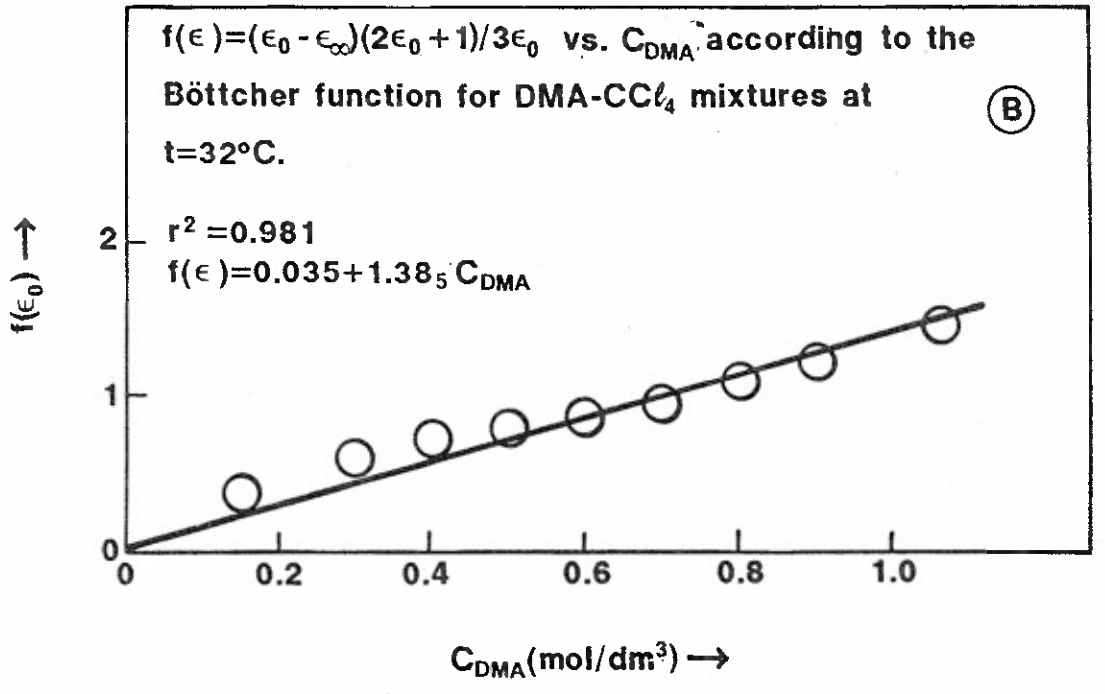
f(ϵ)=(ϵ0 - ϵ∞)(2ϵ0 +1)/3ϵ0 vs. CDMA according to the
Böttcher function for DMA-CCℓ4 mixtures at
t=32°C.
B
r2 =0.981
f(ϵ)=0.035+1.385 CDMA
f(ϵ0) →
CDMA(mol/dm3) →
0
0.2
0.4
0.6
0.8
1.0
1
2

Fig. 3

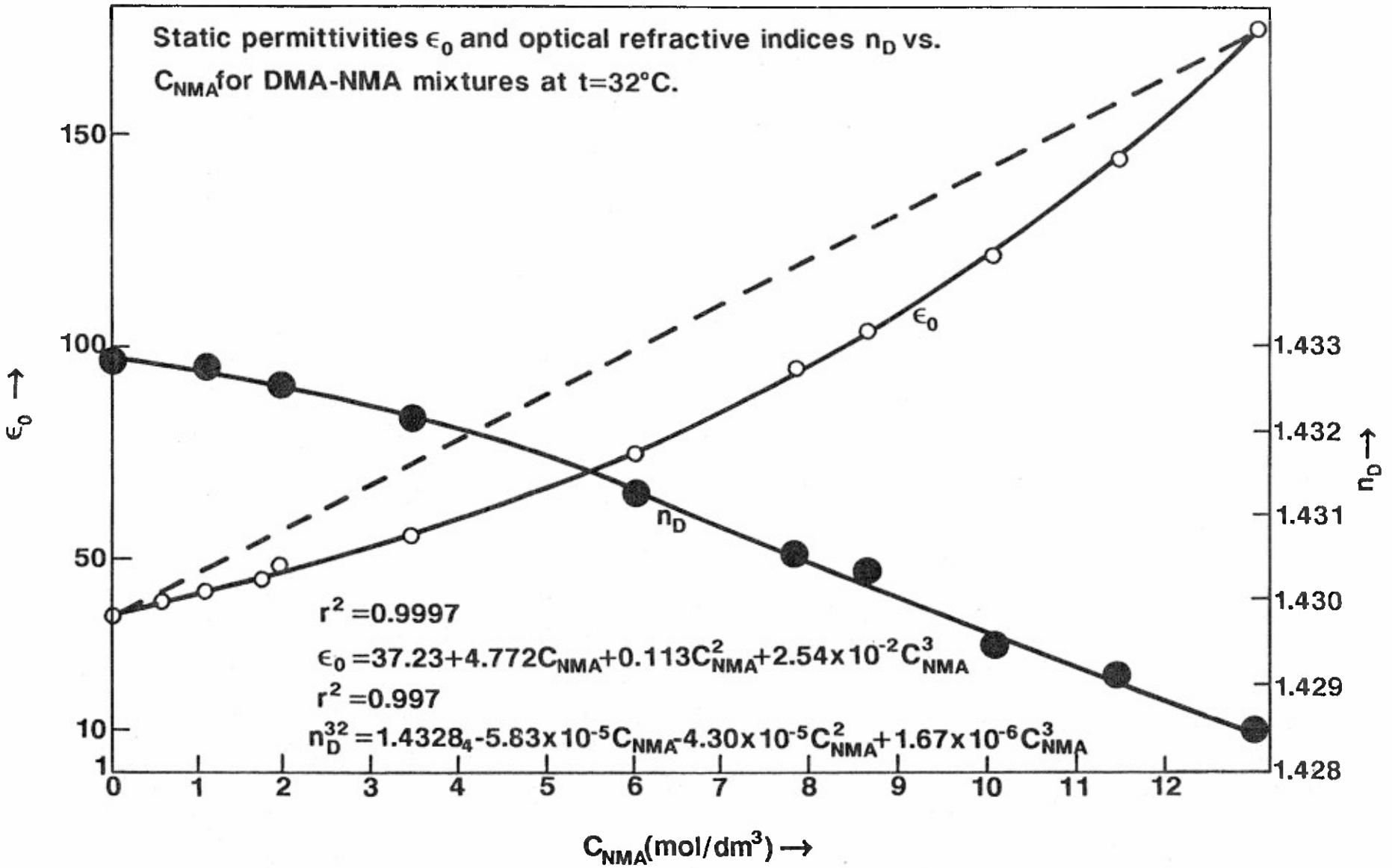
Static permittivities ϵ_0 and optical refractive indices n_D vs.
C_{NMA} for DMA-NMA mixtures at t=32°C.
150
100
50
10
1
ϵ_0 ↑
ϵ_0
n_D
1.433
1.432
1.431
1.430
1.429
1.428
n_D ↑
r^2 =0.9997
ϵ_0 =37.23+4.772C_{NMA}+0.113C^2_{NMA}+2.54x10^{-2}C^3_{NMA}
r^2 =0.997
n_D^{32} =1.4328$_4$-5.83x10^{-5}C_{NMA}-4.30x10^{-5}C^2_{NMA}+1.67x10^{-6}C^3_{NMA}
0 1 2 3 4 5 6 7 8 9 10 11 12
C_{NMA}(mol/dm^3) ⟶

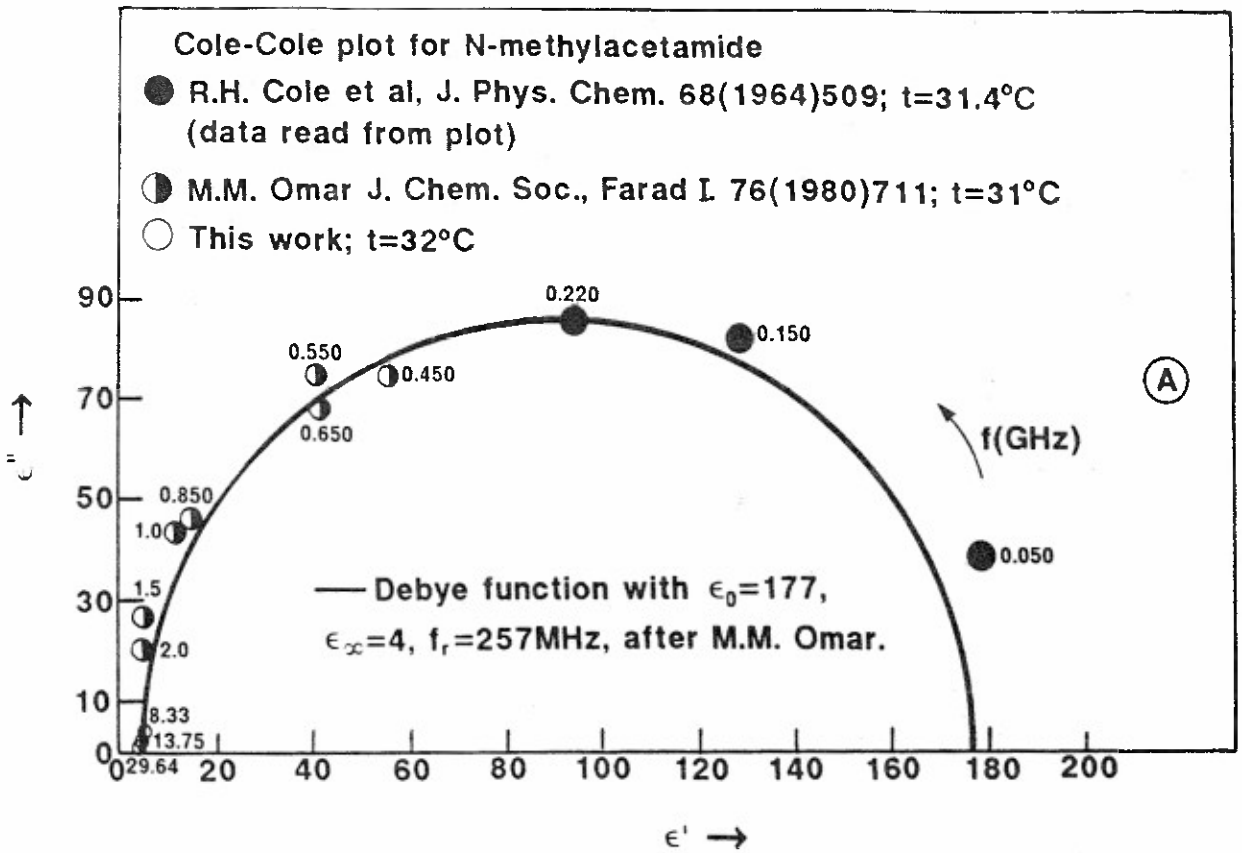
Cole-Cole plot for N-methylacetamide
R.H. Cole et al, J. Phys. Chem. 68(1964)509; t=31.4°C
(data read from plot)
M.M. Omar J. Chem. Soc., Farad I. 76(1980)711; t=31°C
This work; t=32°C
0.220
0.150
0.550
0.450
0.650
0.850
1.0
1.5
2.0
8.33
13.75
29.64
0.050
f(GHz)
A
Debye function with ϵ_0=177,
ϵ_∞=4, f_r=257MHz, after M.M. Omar.
ϵ'' →
ϵ' →

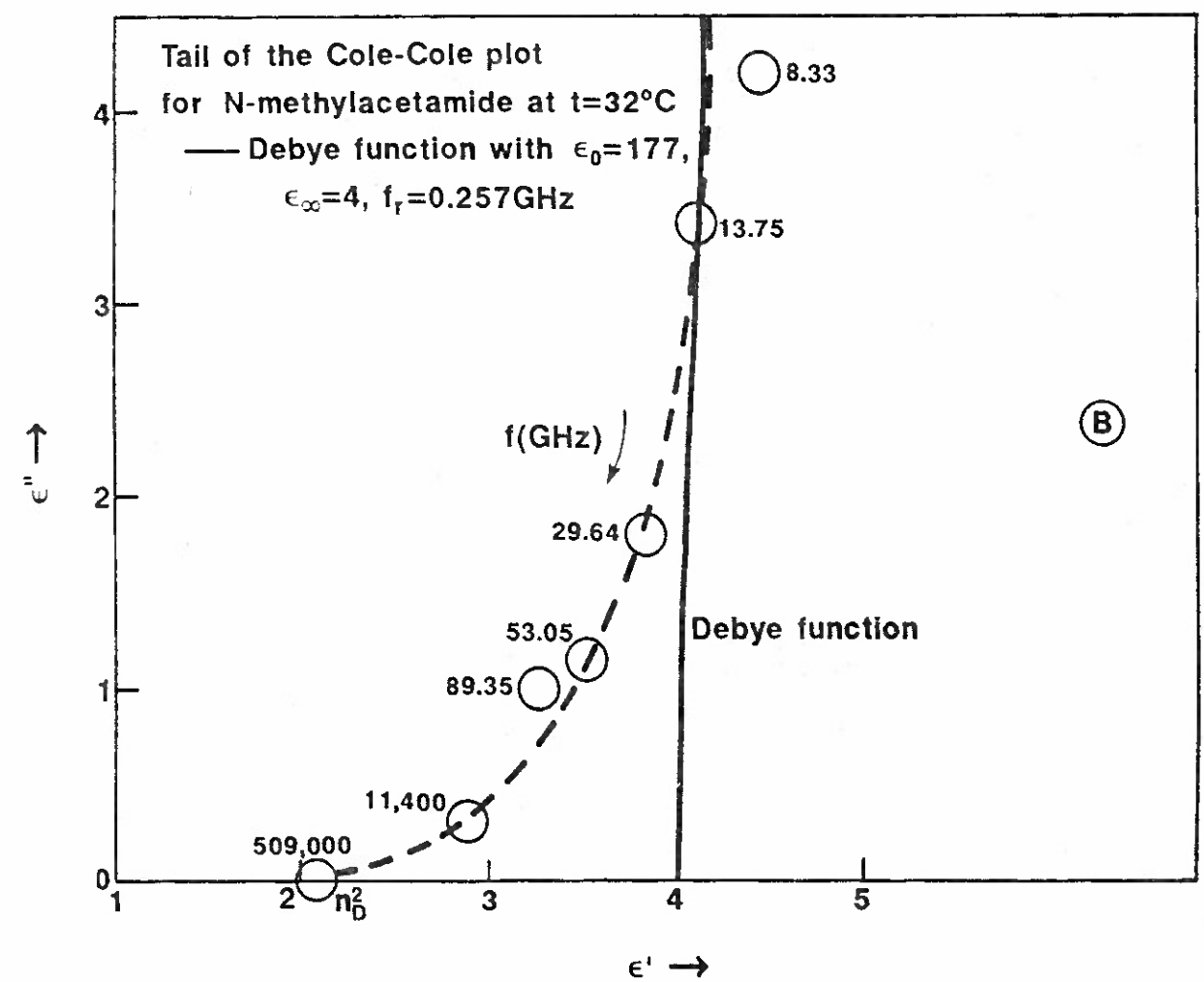
Tail of the Cole-Cole plot
for N-methylacetamide at t=32°C
Debye function with ϵ_0=177,
ϵ_∞=4, f_r=0.257GHz
8.33
13.75
f(GHz)
29.64
53.05
89.35
11,400
509,000
Debye function
B
n_D^2
ϵ'' →
ϵ' →

Fig. 5

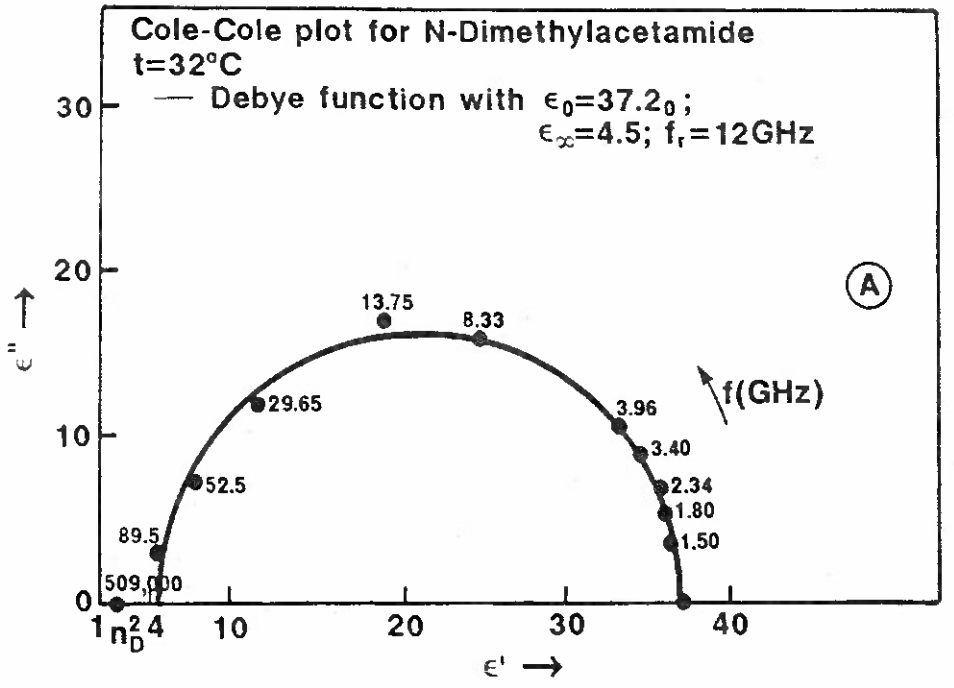
Cole-Cole plot for N-Dimethylacetamide
t=32°C
— Debye function with ϵ_0=37.2$_0$;
ϵ_∞=4.5; f_r=12GHz
A
f(GHz)
13.75
8.33
29.65
3.96
3.40
52.5
2.34
1.80
89.5
1.50
509,000
ϵ''
ϵ' →
n_D^2

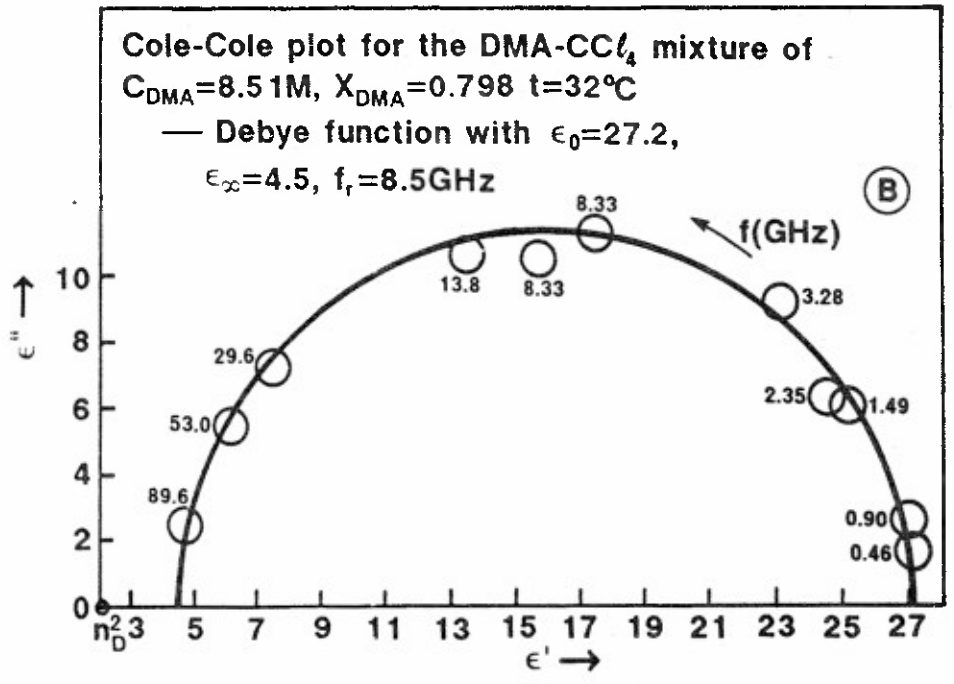
Cole-Cole plot for the DMA-CCℓ_4 mixture of
C_{DMA}=8.51M, X_{DMA}=0.798 t=32°C
— Debye function with ϵ_0=27.2,
ϵ_∞=4.5, f_r=8.5GHz
B
f(GHz)
8.33
13.8
8.33
3.28
29.6
2.35
1.49
53.0
89.6
0.90
0.46
ϵ''
ϵ' →
n_D^2

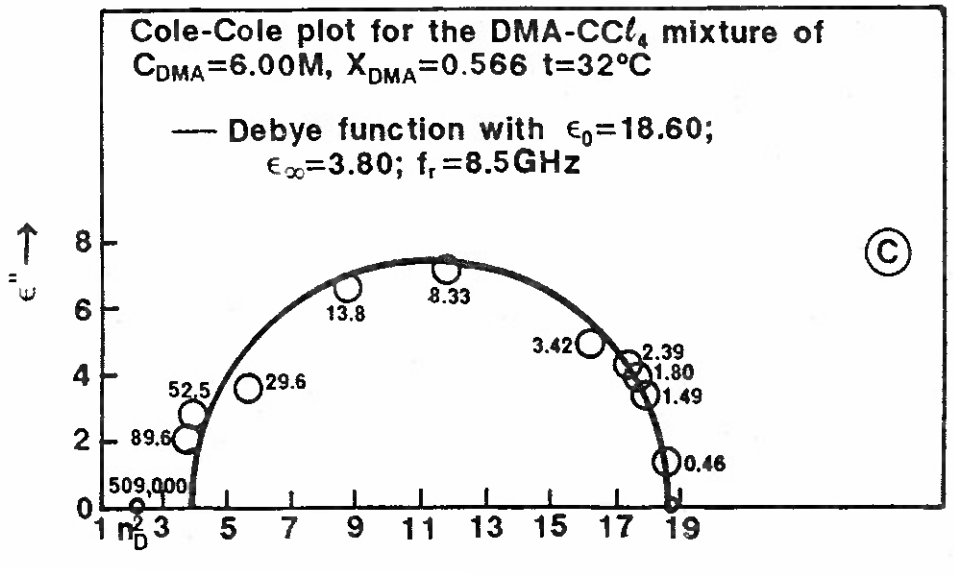
Cole-Cole plot for the DMA-CCℓ_4 mixture of
C_{DMA}=6.00M, X_{DMA}=0.566 t=32°C
— Debye function with ϵ_0=18.60;
ϵ_∞=3.80; f_r=8.5GHz
C
13.8
8.33
3.42
2.39
1.80
52.5
29.6
1.49
89.6
0.46
509,000
ϵ''
n_D^2

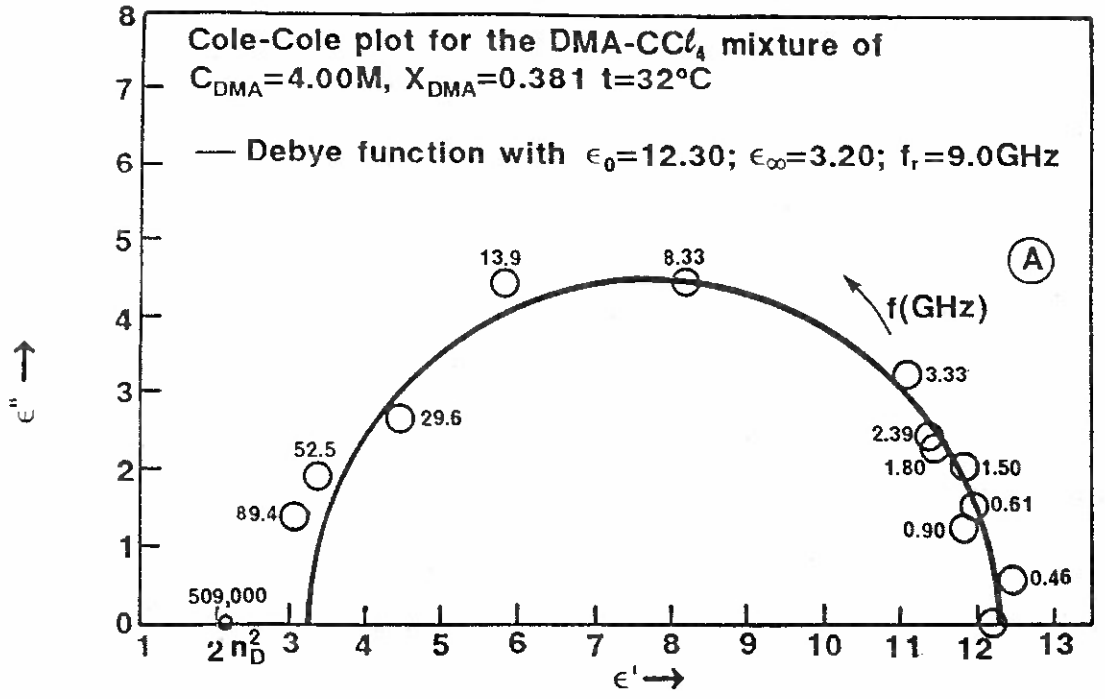
Cole-Cole plot for the DMA-CCl4 mixture of
CDMA=4.00M, XDMA=0.381 t=32°C
— Debye function with ε0=12.30; ε∞=3.20; fr=9.0GHz
A
f(GHz)
13.9
8.33
3.33
29.6
2.39
52.5
1.80
1.50
89.4
0.61
0.90
0.46
509,000
2 nD2
ε' →
ε" →

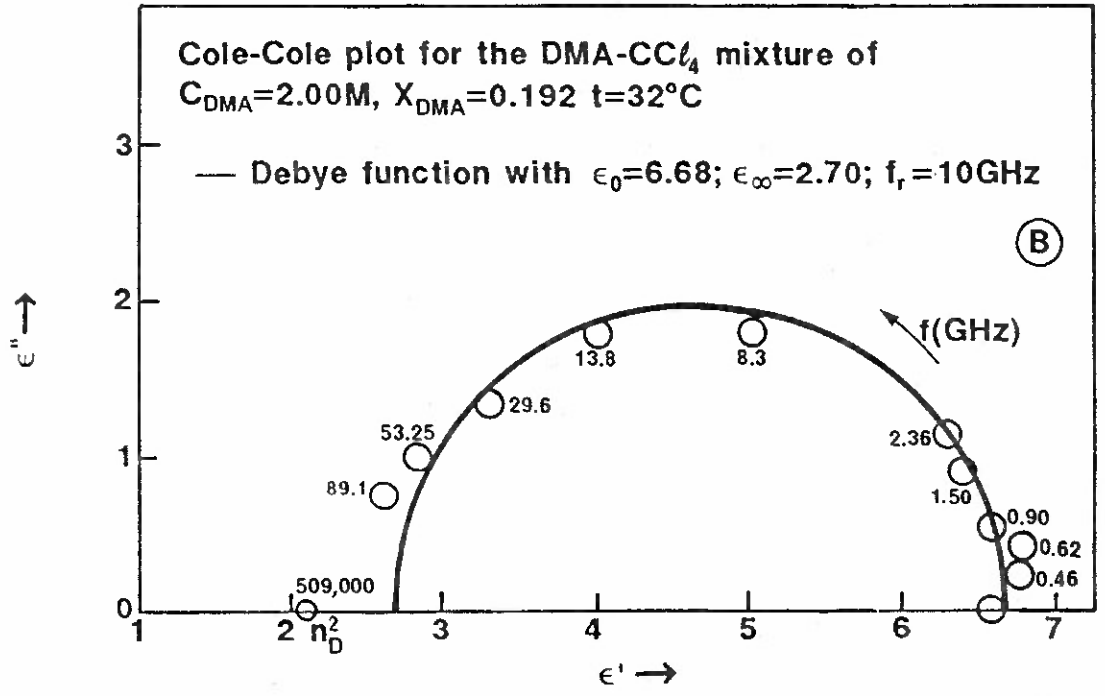
Cole-Cole plot for the DMA-CCl4 mixture of
CDMA=2.00M, XDMA=0.192 t=32°C
— Debye function with ε0=6.68; ε∞=2.70; fr=10GHz
B
f(GHz)
13.8
8.3
29.6
53.25
2.36
89.1
1.50
0.90
0.62
0.46
509,000
2 nD2
ε' →
ε" →

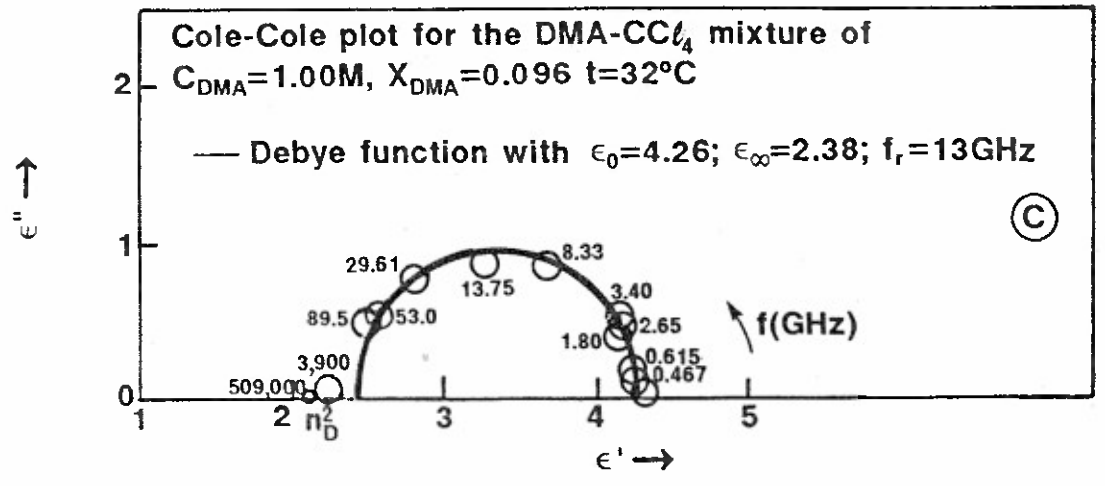
Cole-Cole plot for the DMA-CCl4 mixture of
CDMA=1.00M, XDMA=0.096 t=32°C
— Debye function with ε0=4.26; ε∞=2.38; fr=13GHz
C
f(GHz)
29.61
13.75
8.33
3.40
89.5
53.0
2.65
1.80
0.615
0.467
3,900
509,000
2 nD2
ε' →
ε" →

Fig.7

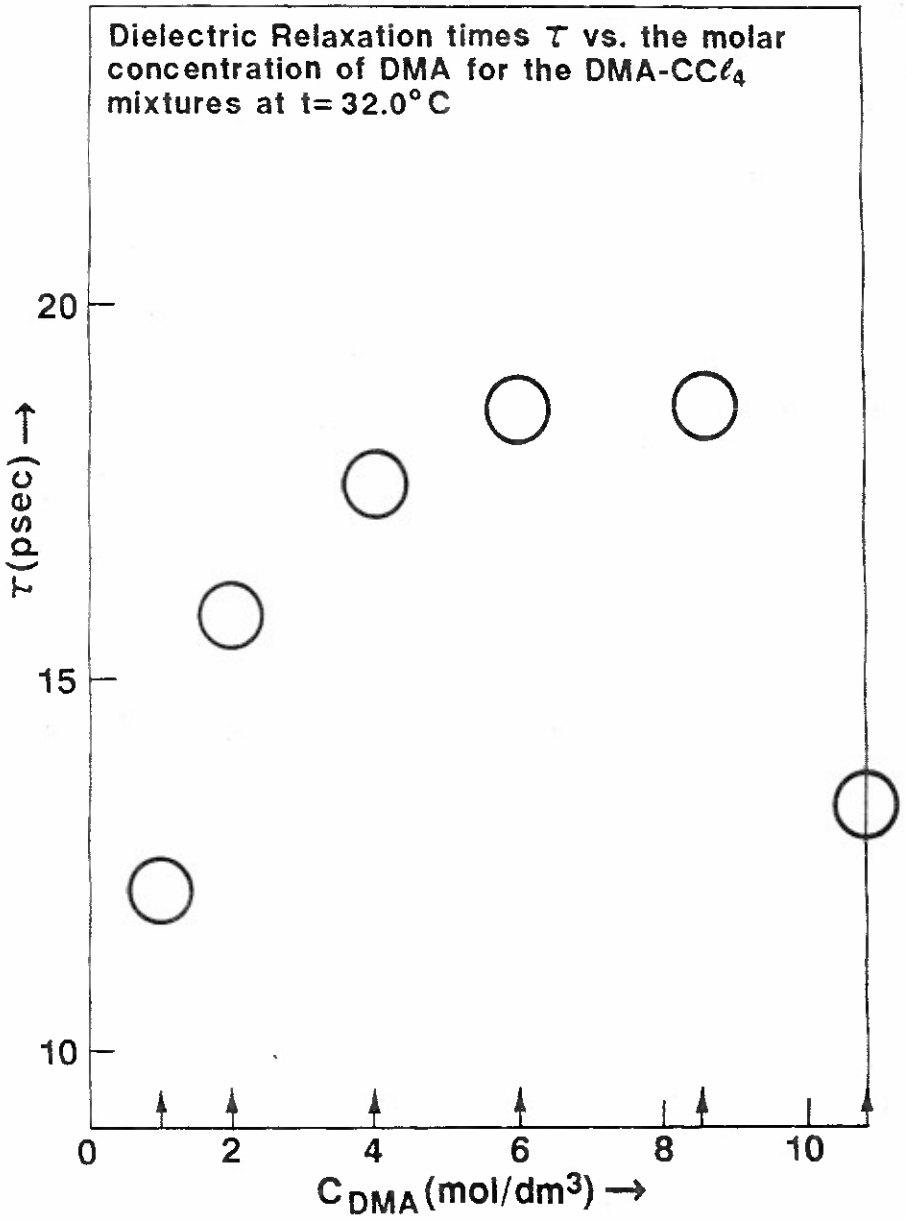
Dielectric Relaxation times τ vs. the molar concentration of DMA for the DMA-CCℓ4 mixtures at t= 32.0° C
20
15
10
τ(psec) →
0
2
4
6
8
10
C DMA (mol/dm3) →

Fig. 8

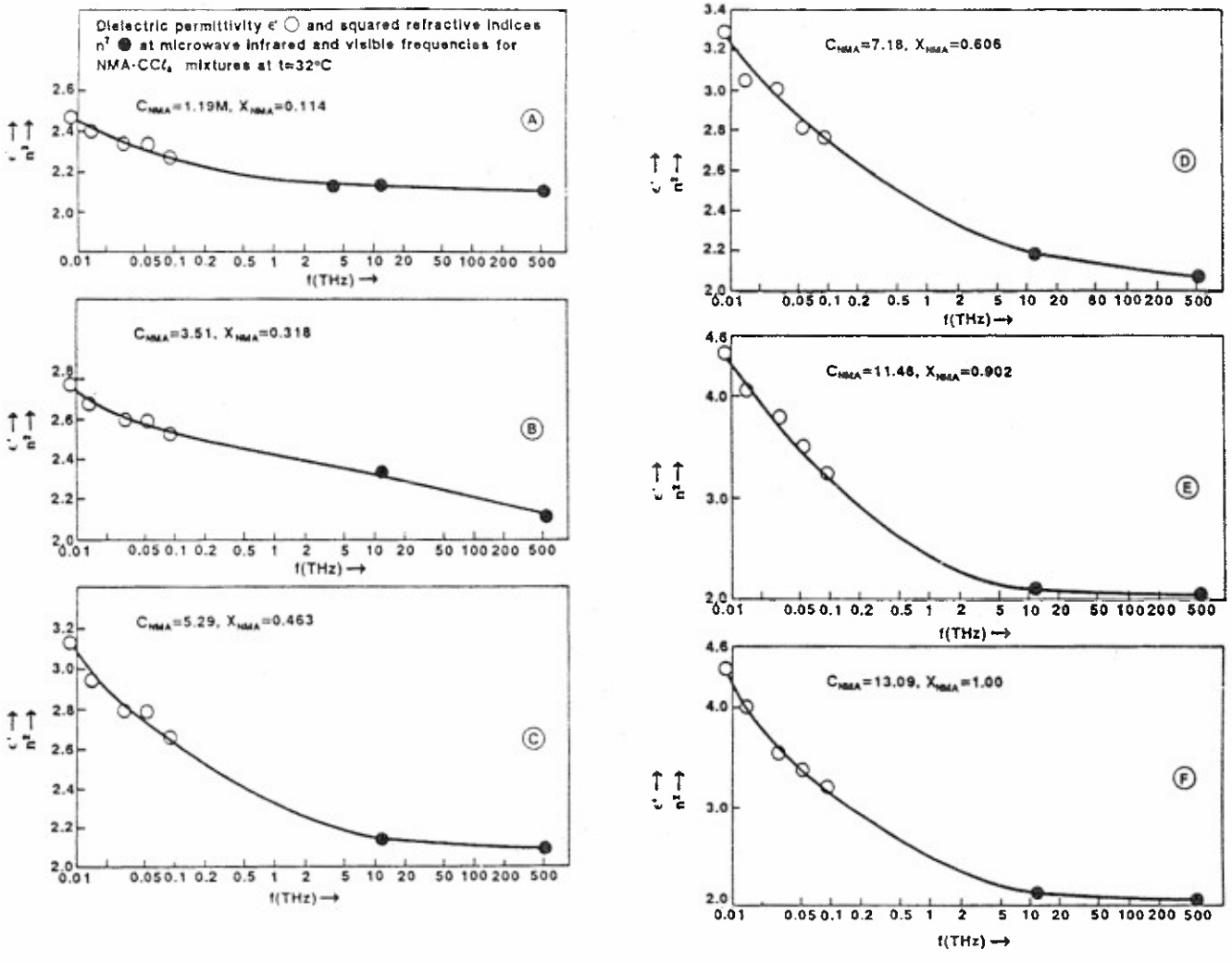
Dielectric permittivity ε' ○ and squared refractive indices n² ● at microwave infrared and visible frequencies for NMA·CCℓ₄ mixtures at t=32°C
C_NMA=1.19M, X_NMA=0.114
A
C_NMA=3.51, X_NMA=0.318
B
C_NMA=5.29, X_NMA=0.463
C
C_NMA=7.18, X_NMA=0.606
D
C_NMA=11.48, X_NMA=0.902
E
C_NMA=13.09, X_NMA=1.00
F
f(THz) →
0.01 0.05 0.1 0.2 0.5 1 2 5 10 20 50 100 200 500

Fig. 9

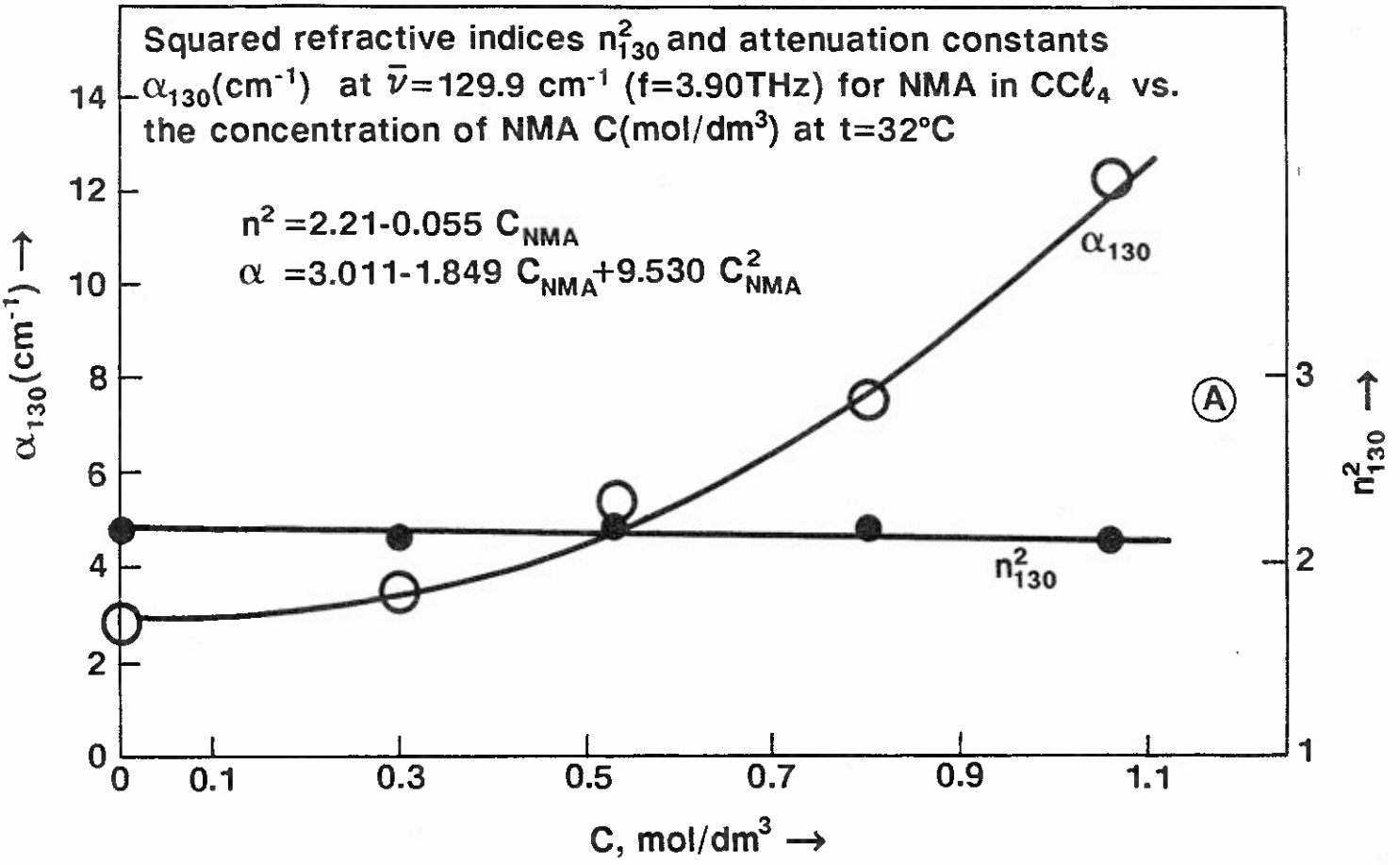
Squared refractive indices n^2_{130} and attenuation constants $\alpha_{130}(cm^{-1})$ at $\bar{\nu}$=129.9 cm^{-1} (f=3.90THz) for NMA in $CC\ell_4$ vs. the concentration of NMA C(mol/dm³) at t=32°C
n^2 =2.21-0.055 C_{NMA}
α =3.011-1.849 C_{NMA}+9.530 C^2_{NMA}
α_{130}
n^2_{130}
A
$\alpha_{130}(cm^{-1})$ →
n^2_{130} →
C, mol/dm³ →
0 0.1 0.3 0.5 0.7 0.9 1.1
0 2 4 6 8 10 12 14
1 2 3

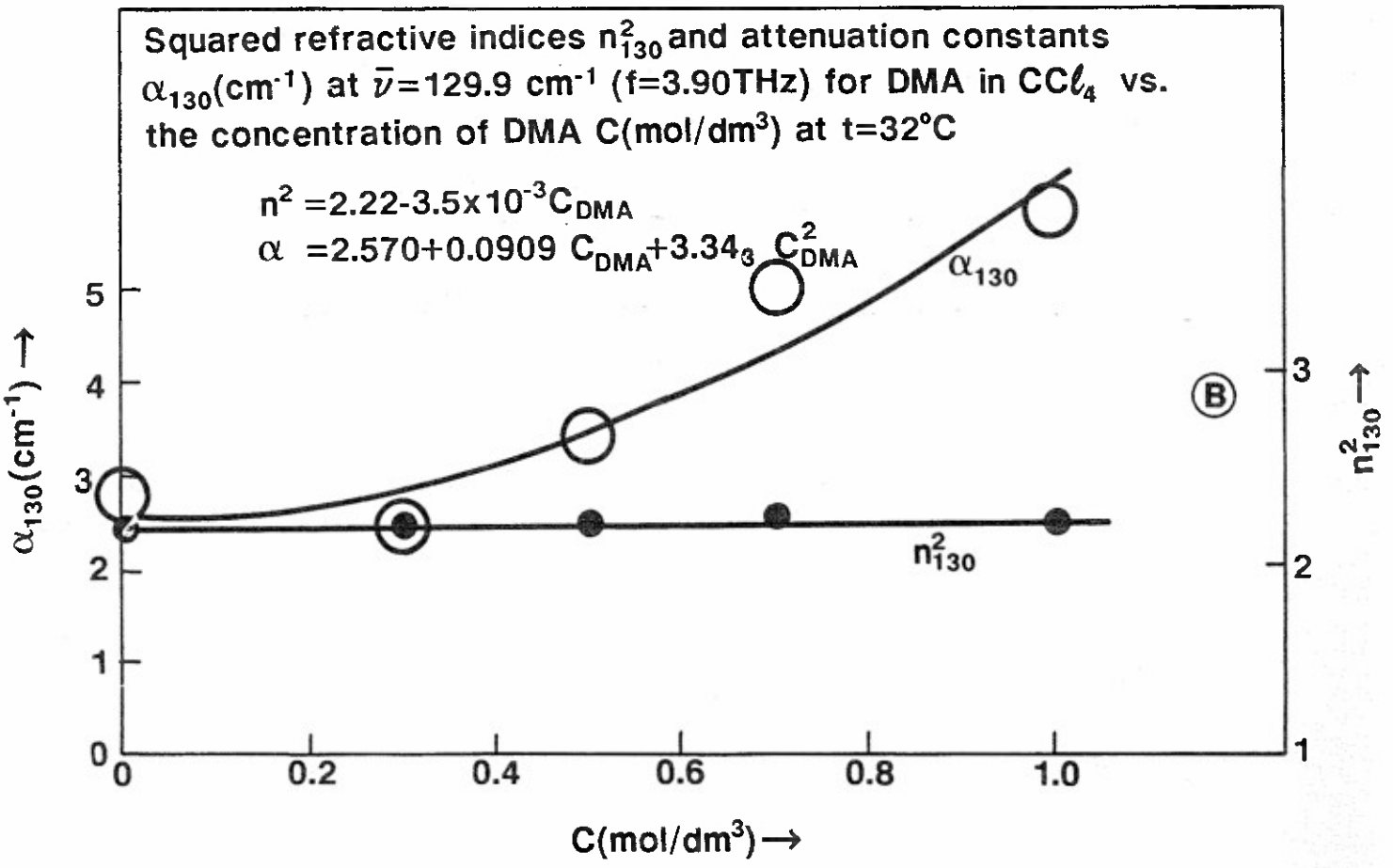
Squared refractive indices n^2_{130} and attenuation constants $\alpha_{130}(cm^{-1})$ at $\bar{\nu}$=129.9 cm^{-1} (f=3.90THz) for DMA in $CC\ell_4$ vs. the concentration of DMA C(mol/dm³) at t=32°C
n^2 =2.22-3.5x10^{-3}C_{DMA}
α =2.570+0.0909 C_{DMA}+3.34$_3$ C^2_{DMA}
α_{130}
n^2_{130}
B
$\alpha_{130}(cm^{-1})$ →
n^2_{130} →
C(mol/dm³) →
0 0.2 0.4 0.6 0.8 1.0
0 1 2 3 4 5
1 2 3

Fig. 10